

Stability of the Larsen B ice shelf on the Antarctic Peninsula during the Holocene epoch

Eugene Domack¹, Diana Duran¹, Amy Leventer², Scott Ishman³, Sarah Doane¹, Scott McCallum³, David Amblas⁴, Jim Ring⁵, Robert Gilbert⁶ & Michael Prentice⁷

The stability of the Antarctic ice shelves in a warming climate has long been discussed¹, and the recent collapse of a significant part, over 12,500 km² in area, of the Larsen ice shelf off the Antarctic Peninsula^{2,3} has led to a refocus toward the implications of ice shelf decay for the stability of Antarctica's grounded ice^{4–6}. Some smaller Antarctic ice shelves have undergone periodic growth and decay over the past 11,000 yr (refs 7–11), but these ice shelves are at the climatic limit of ice shelf viability¹² and are therefore expected to respond rapidly to natural climate variability at century to millennial scales^{8–11}. Here we use records of diatoms, detrital material and geochemical parameters from six marine sediment cores in the vicinity of the Larsen ice shelf to demonstrate that the recent collapse of the Larsen B ice shelf is unprecedented during the Holocene. We infer from our oxygen isotope measurements in planktonic foraminifera that the Larsen B ice shelf has been thinning throughout the Holocene, and we suggest that the recent prolonged period of warming in the Antarctic Peninsula region^{13,14}, in combination with the long-term thinning, has led to collapse of the ice shelf.

A marine geologic survey was conducted in the northwestern Weddell Sea (between 65° S and 66° S, and 59° W and 61° W) just before the dramatic collapse of a large portion of the Larsen ice shelf B (LIS-B; colloquially Larsen B ice shelf) in March 2002 (Fig. 1). Here we collected sediment cores, surface sediment grabs, bottom photographs and oceanographic profiles of temperature and salinity, and conducted a reconnaissance bathymetric survey (Figs 2 and 3). These data were collected in open water just east of the pre-collapse LIS-B front, but following a series of calving events resulting in shelf edge retreat before the 2002 collapse. Thus the LIS-B cores and an additional core¹¹ previously collected in the LIS-A region (core 23 in Fig. 1a) were located in a sub-ice shelf setting until 1995. Surface phytoplankton concentrations were estimated via ocean colour satellite imagery (Fig. 1c) and surface water sampling. The sediment cores recovered glacial and Holocene marine sedimentary sequences representing the transitions from glacial conditions to de-glacial (sub-ice shelf) conditions, and then to open marine conditions. Three stratigraphic intervals (units 3, 2 and 1) are recognized: a lower homogeneous diamicton (unit 3; glacial), a stratified to cross-stratified gravelly sand to granulated mud (unit 2; deglacial), and an upper laminated to homogeneous, slightly sandy mud (unit 1; sub-ice shelf) (Fig. 2b). Only the uppermost centimetre of unit 1, with higher biosiliceous content, represents open marine conditions. These units are interpreted on the basis of a number of specific criteria in Antarctic glacial marine sequences^{11,15,16}. The presence of glacial till (unit 3) is consistent with the glacially sculpted and streamlined sea floor documented from multibeam data (Fig. 1b)

and with a much expanded glacial regime on both sides of the Antarctic Peninsula (Fig. 1a; see Supplementary Information).

Termination of glacial cover upon the sea floor of both LIS-A and LIS-B is constrained by radiocarbon dates of $10,600 \pm 55$ years before present (yr BP) on calcareous foraminifera within the base of the sub-ice shelf facies, unit 1 in core KC-2 (Table 1), and palaeomagnetic intensity cross-dates of $10,700 \pm 500$ yr BP within LIS-A cores¹¹. Radiocarbon ages on calcareous foraminifera and organic matter (Table 1) demonstrate that subsequent deposition beneath the LIS-B took place at progressively lower rates following deglaciation. In support of lithofacies interpretations is the twofold greater thickness for unit 1 within core KC-3, when compared to other cores (Fig. 2b). KC-3 is closest to the historical grounding line of the LIS-B around Jason Peninsula (Fig. 1b) and would be expected to have received glacial detritus at greater rates than sites more distal from the debris source (the grounding line).

All of the cores except KC-3 are characterized by concentrations of gravel at the sediment–water interface (Fig. 2a) marking the accumulation of coarse ice-rafted material. This is a result of a combination of coarse debris released when the ice shelf retreated to its penultimate position in 1998¹⁵ and the rafting of poorly sorted stones under the distal reaches of the LIS-B, which was generally devoid of material except for englacial debris septa entrained at tributary junctures along the Antarctic Peninsula¹⁷. The inference that some of these stones resided exposed on the sea floor for some time is supported by the MnO₂ coatings of a few micrometres thickness over their surface, requiring at least 1.5–2.7 kyr to accumulate given observed rates of MnO₂ accretion in the Southern Ocean¹⁸. The surface of unit 1 is not a winnowed or lag surface but one of low sedimentation (Table 1) as ²¹⁰Pb activities show near-surface excess beyond background levels (Fig. 3b), albeit associated with very low sediment accumulation rates (Table 1). Only a few of the large boulders recovered and observed in bottom photographs (Fig. 2b) show evidence of recent colonization by epifaunal organisms. All such organisms yield modern ¹⁴C ages for biogenic calcite (Table 1, AA-49353 to AA-49358), attesting to the recent increase in advection of organic detritus to the sea floor in this area. Extremely low diatom abundance within all except the upper centimetre of unit 1 supports a sub-ice shelf origin for unit 1.

Quantitative downcore diatom data (Fig. 3a) indicate contrasting Holocene histories for LIS-A and LIS-B. It is notable that there is a much higher overall diatom concentration in KC23 (LIS-A) as contrasted to concentrations in LIS-B cores, which are several orders of magnitude lower, reinforcing the hypothesis that while the LIS-A region had no ice shelf for extended periods during the Holocene¹¹, the LIS-B persisted through the Holocene until its recent collapse. A significant increase in absolute diatom concentration noted in some

¹Department of Geosciences, Hamilton College, Clinton, New York 13323, USA. ²Department of Geology, Colgate University, Hamilton, New York 13346, USA. ³Department of Geology, Southern Illinois University, Carbondale, Illinois 62901, USA. ⁴Department of Stratigraphy, Paleontology, and Marine Geosciences, University of Barcelona, 08028 Barcelona, Spain. ⁵Physics Department, Hamilton College, Clinton, New York 13323, USA. ⁶Department of Geography, Queen's University, Kingston, Ontario ON K7L 3N6, Canada. ⁷Department of Earth Science, University of New Hampshire, Durham, New Hampshire 03824, USA.

surface sediments from LIS-B illustrates the impact of very recent ice shelf breakout on underlying sediments (Fig. 3a). The heterogeneous nature of the sea-floor surface (Fig. 2a) and the short duration over which open water has existed in this area account for the heterogeneity of surface diatom peaks. These modern values are orders of magnitude lower than values recorded from other parts of the western Weddell Sea shelf¹⁹, reflecting relatively low annual production in a region still characterized by high seasonal sea ice concentration. Surface sediment diatom assemblages, including *Fragilariopsis curta*, document an environment dominated by sea ice. The valves are lightly silicified; reinforcing that dissolution is not the principal reason for low diatom abundances in LIS-B surface sediments.

Apart from the upper centimetre, sparse diatom valves and fragments occur within unit 1, attributed to advection and deposition under the ice shelf, as observed under other ice shelves²⁰. Phytoplankton and surface chlorophyll concentrations from satellite data demonstrate a large algal bloom east of the ice front which, together with the observed bottom current trajectories (Figs 1c and 2a), support the potential for advection of biogenic components underneath the ice shelf. The distinct increase in foraminiferal abundance in unit 1 is paralleled by diatom data;

while low concentrations of diatoms are found in unit 1, even diatom fragments are nearly absent in unit 2, and are indeed completely lacking in unit 3.

Finally, the petrologic composition of terrigenous grains within the sediment cores indicate only subtle shifts in debris provenance consistent with sub-glacial to sub-ice shelf deposition, and a source limited to substrates eroded upstream of glacial or ice shelf flow^{10,16,21} (Supplementary Information). Exotic iceberg rafted detritus is a key characteristic in recognition of open marine versus sub-ice shelf palaeoenvironments^{10,11,16}.

All the evidence indicates that LIS-B has been a stable component of the northwestern Weddell Sea since the Late Pleistocene to Holocene transition, 11.5 kyr BP. In contrast, the northernmost portions of a much larger Larsen ice shelf system and small ice shelves on the western side of the Antarctic Peninsula experienced periods of decay and open marine conditions during the Holocene^{7–11,15}. Our observation, that the modern collapse of the LIS-B is a unique event within the Holocene, supports the hypothesis that the current warming trend in the northwestern Weddell Sea has exceeded past warm episodes in both its magnitude and duration.

The suggestion that the LIS has recently experienced accelerated thinning due to under-melt²² may also help explain the unique

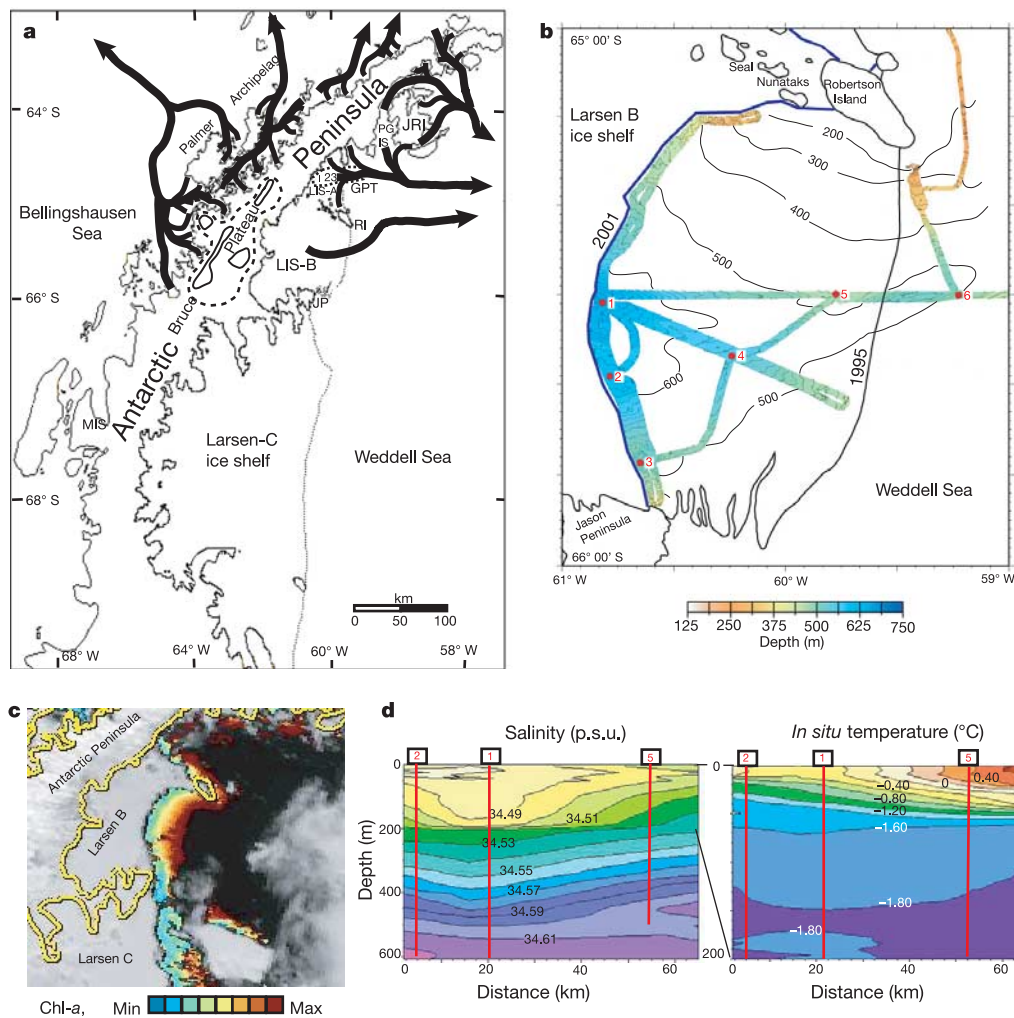


Figure 1 | Location maps, satellite imagery and ocean profiles. **a**, Study area along the northern Antarctic Peninsula, showing reconstructed ice flow lines (arrows), and Larsen A ice shelf (LIS-A), Larsen B ice shelf (LIS-B), Müller ice shelf (MIS), Robertson island (RI), Greenpeace trough (GPT), James Ross island (JRI), Prince Gustav ice shelf (PGIS), and location of core KC-23 (see Fig. 3). Bruce plateau shows proposed (dashed line) extent of high

elevation ice dome and includes modern ice domes of low elevation (solid line). **b**, Bathymetry and core locations (red dots) with positions of LIS-B in 1995 and late 2001 indicated. **c**, Sea surface chlorophyll-*a* (chl-*a*) concentrations from satellite (SeaWiFS) imagery collected on 11 December 2001. **d**, Contoured sections of ocean temperature and salinity from vertical profiles (stations as in **b**).

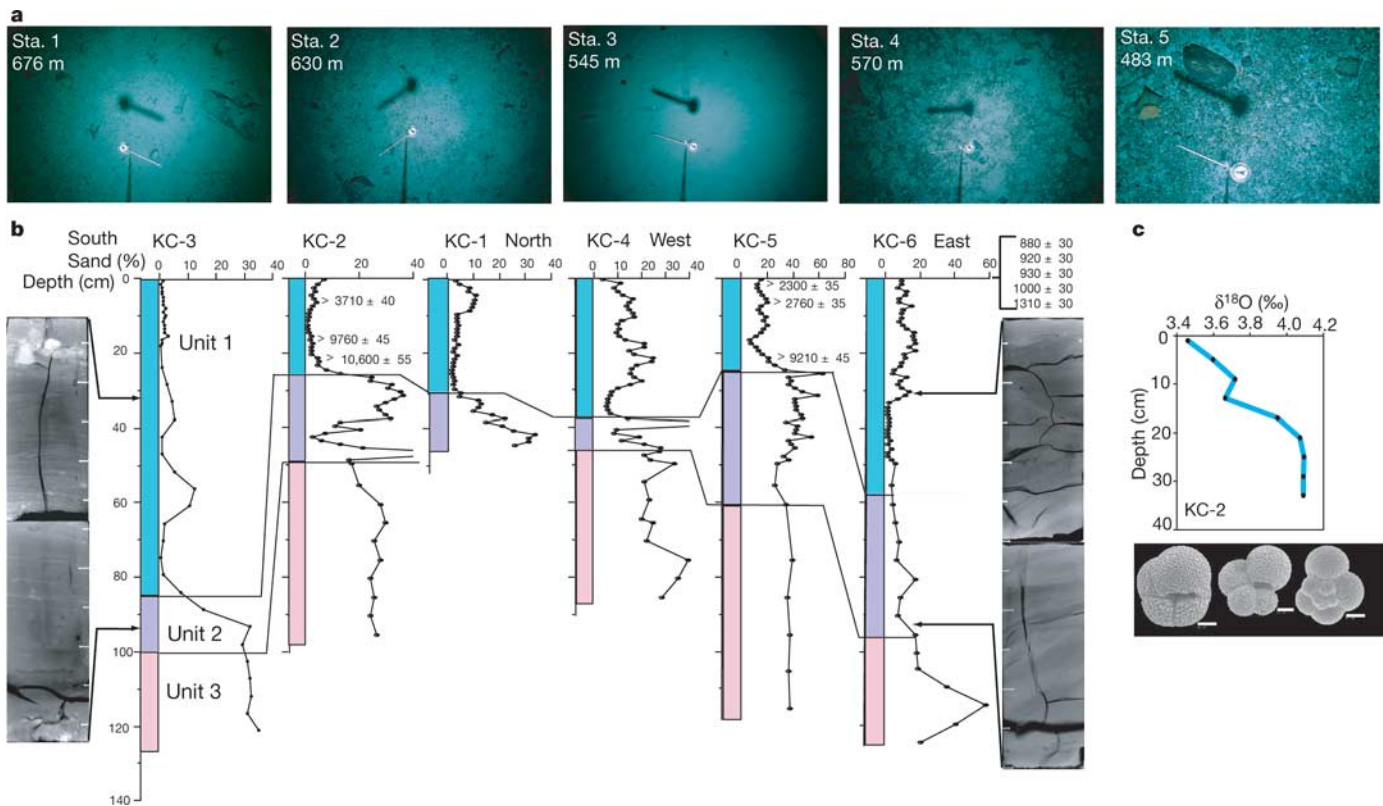


Figure 2 | Bottom photographs and core stratigraphy for sea-floor stations within the Larsen B embayment. **a**, Photographs with current vane and compass for stations 1, 2, 3, 4 and 5. **b**, Stratigraphic fence diagram of kasten cores 1–6 (see Fig. 1b), illustrating sand content, divisions between units 1, 2 and 3, and X-ray radiography negatives for portions of cores 3 and 6.

Uncorrected radiocarbon ages (see Table 1) are shown for biogenic calcite for indicated depths within cores 2 and 5 and for epibenthic organisms at surface of station 6. **c**, Oxygen isotopes on two forms of *Neogloboquadrina pachyderma* (SEM image scale bar is 80 μm for left image, and 60 μm for middle and right image).

history of the LIS-B. A thick LIS-B following ice sheet decoupling could have provided a significant buffer to the water hammer process whereby ice shelves disintegrate¹³. Basal melt rates of 0.78 m yr^{-1} estimated for the LIS-B²² are crucial to this argument, in that LIS-B could not have been sustained through the Holocene without calling on an initial ice shelf that was unrealistically thick or on equally unreasonable flow velocities. It is unlikely that relatively warm ocean waters at any time in the past interacted with the melt regime of the LIS-B. Instead, we propose a slow, steady reduction of ice shelf thickness by a few tens of metres as a response to the natural drawdown of the glacial profile following deglaciation. With continued flow and drainage of ice formed during the Latest Pleistocene

(Fig. 1a), as well as recent under-melting and/or densification²², the LIS-B eventually thinned to the point where it too succumbed to the prolonged period of regional warming now affecting the entire Antarctic Peninsula region^{13,14}.

Oxygen isotopes from planktonic foraminifera (Fig. 2c) provide evidence of progressive melt effects within the water column beneath the LIS-B. Over the last 10 kyr a 0.8‰ enrichment of $\delta^{18}\text{O}$ is observed. This is consistent with a combination of ice volume effects for the Holocene (about 0.6‰)^{23,24} and a slight freshening of the water column consistent with limited under-melt. Temperature changes are not responsible for the shift in $\delta^{18}\text{O}$ because the waters today are already close to freezing²⁵ (Fig. 2d) and could not have been

Table 1 | Radiocarbon ages from sediment samples acquired during NBP01-07

Laboratory number	Core depth (cm)	Uncorrected ^{14}C age (yr)	$\delta^{13}\text{C}$ of carbon (‰)	Interval sedimentation rate (mm yr^{-1})	Organic carbon source
AA-49355	G-6 (0)	880 \pm 30	0.10		Foraminifera
AA-49357	G-6 (0)	920 \pm 30	0.80		Coral
AA-49358	G-6 (0)	930 \pm 30	1.50		Bryozoan
AA-49353	G-6 (0)	1,000 \pm 30	0.40		Serpulid
AA-49356	G-6 (0)	1,310 \pm 30	0.80		Brachiopod
AA-49359	KC-5 (0–2)	9,360 \pm 100	–23.40	–	a.i.o.m.
AA-49360	KC-5 (12–14)	13,930 \pm 120	–23.60	0.028	a.i.o.m.
AA-49361	KC-5 (24–25)	18,680 \pm 170	–23.70	0.021	a.i.o.m.
NO-38246	KC-5 (0–2)	2,300 \pm 35	1.03	0.007	Foraminifera
NO-39000	KC-5 (4–6)	2,760 \pm 35	0.91	0.088	Foraminifera
NO-39001	KC-5 (20–22)	9,210 \pm 45	0.92	0.025	Foraminifera
NO-38996	KC-2 (4–6)	3,710 \pm 40	0.56	0.018	Foraminifera
NO-38244	KC-2 (16–18)	9,760 \pm 45	0.35	0.020	Foraminifera
NO-38245	KC-2 (20–22)	10,600 \pm 55	–0.05	0.048	Foraminifera

a.i.o.m., acid insoluble organic matter.

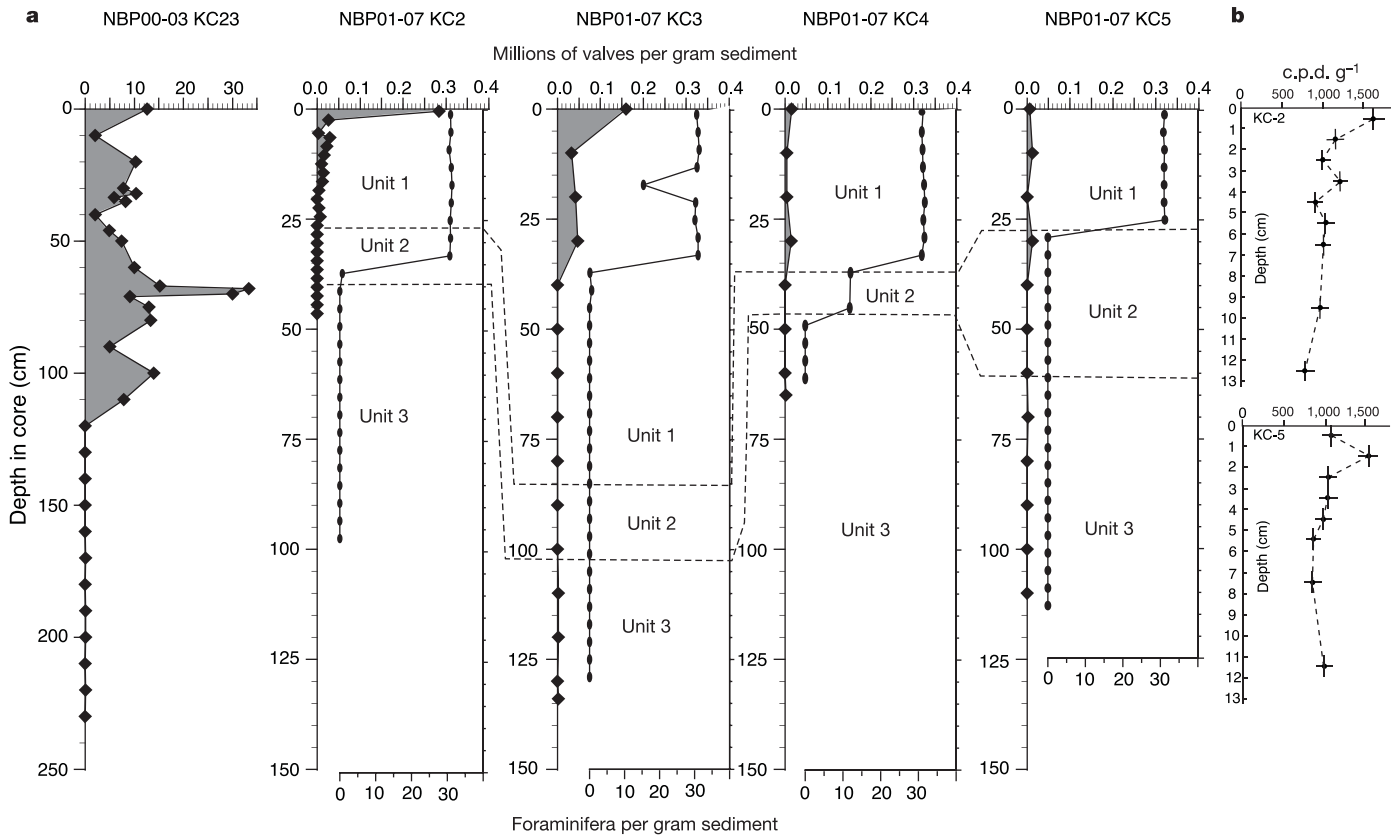


Figure 3 | Microfossil abundance and radioactive ^{210}Pb activity within marine sediment cores from beneath the Larsen ice shelf. **a**, Stratigraphic abundance of diatom valves (top scale, diamonds) and foraminifera (bottom scale, ellipses) with stratigraphic unit divisions (see Figs 1b and 2b). **b**, ^{210}Pb

activities for near surface samples in cores 2 and 5 (units on x axis for ^{210}Pb data are counts per day per gram (c.p.d. g^{-1}). Error bars for the ^{210}Pb data represent the sample depths (1 cm) and counting statistics based on a Poisson distribution and incremental background measurements.

significantly colder during the Holocene. Oceanographic data collected along the front of the LIS-B in December 2001 show a lens of sub-ice shelf melt water consistent with, at most, a few centimetres of under-melt beneath the ice shelf²⁶ (Fig. 1d).

Direct geologic evidence from beneath the LIS-B indicates that the recent break-up event is unprecedented in the Holocene history of this glacial system. The ice shelf's demise is probably the consequence of a combination of long term thinning (by a few tens of metres) over thousands of years and short term (multi-decadal) cumulative increases in surface air temperature that have exceeded the natural variation of regional climate during the Holocene interglacial.

METHODS

Field methods. Cores, water samples, bottom photographs and oceanographic data were collected during US Antarctic Program cruise 2001-07 of the *Nathaniel B. Palmer* (see <http://www.hamilton.edu/news/exp/Antarctica2001/> for details).

Diatom analyses. Quantitative diatom slides were prepared using a settling method²⁷ that produces a random distribution of diatoms and allows calculation of absolute diatom abundances. Diatoms were counted along transects at $400\times$ magnification on an Olympus BX60 microscope. Between 5 and 10 transects were counted for each sample.

Radioisotope dating. The chronology of radiocarbon dates in Antarctica depends upon an assumption of a large reservoir correction (~ 1.2 kyr) and adjustments for reworking of organic matter¹⁶. We avoid the later problem by using calcareous foraminifera (Fig. 2c), listing all ages as uncorrected for reservoir age, and providing living ages (reservoir age estimate) on modern calcite from the locale (Table 1). The ages reported in Table 1 are corrected only for the $\delta^{13}\text{C}$ fractionation and are not calibrated. Processing of samples follows established procedures^{15,16}. Interval sedimentation rates are calculated from ages between adjacent stratigraphic levels and are provided for both calcite and acid insoluble organic matter (a.i.o.m.) samples. ^{14}C analyses were completed at the

University of Arizona (AA) and the National Ocean Sciences Accelerator Mass Spectrometer facility at Woods Hole Oceanographic Institution (NO). ^{210}Pb methods followed published procedures²⁸.

Manganese oxide. Eleven thickness measurements of MnO_2 , ranging from 4.2 to $16.7\ \mu\text{m}$, were determined from thin sections of clasts collected at site 5. We used a FEI Quanta scanning electron microscope integrated with an EDAX Phoenix energy dispersive spectrometer. The modal thickness of MnO_2 coating was 3–6 μm with a mean value of 9.4 μm . We then compared the mean thicknesses to published rates (and means) of MnO_2 accretion near the Weddell Sea¹⁸ to provide an estimate for the duration of exposure as between 1.5 and 2.7 kyr.

Grain lithology. Supplementary Data illustrate downcore petrographic assignment of the gravel to coarse sand fraction from sample intervals in core 5 (Fig. 2b). Gravel and coarse sand fractions were removed from matrix by wet sieving, and grain counts were made by examination under a binocular microscope.

Glacial reconstruction. Ice sheet flow directions and reconstructions (Fig. 1c) were based upon a compilation of published information on swath bathymetry for regions surrounding the northern Antarctic Peninsula (Supplementary Information). Details of sea-floor relief for the LIS-B region are confirmed by comparisons of our data (Fig. 1b) to published information²⁹.

Received 16 December 2004; accepted 7 June 2005.

1. Mercer, J. H. West Antarctic ice sheet and CO_2 greenhouse effect: a threat of disaster. *Nature* **271**, 321–325 (1978).
2. Vaughan, D. G. & Doake, C. S. M. Recent atmospheric warming and retreat of ice shelves on the Antarctic Peninsula. *Nature* **379**, 328–331 (1996).
3. Scambos, T., Hulbe, C. & Fahnestock, M. Climate-induced ice shelf disintegration in the Antarctic Peninsula. *Antarct. Res. Ser.* **79**, 79–92 (2003).
4. De Angelis, H. & Skvarca, P. Glacier surge after ice shelf collapse. *Science* **299**, 1560–1562 (2003).
5. Scambos, T. A., Bohlander, J. A., Shuman, C. A. & Skvarca, P. Glacier acceleration and thinning after ice shelf collapse in the Larsen B embayment, Antarctica. *Geophys. Res. Lett.* **31**, L18402, doi:10.1029/2004GL020670 (2004).

6. Rignot, E. *et al.* Accelerated ice discharge from the Antarctic Peninsula following the collapse of Larsen B ice shelf. *Geophys. Res. Lett.* **31**, L18401, doi:10.1029/2004GL020697 (2004).
7. Clapperton, C. M. & Sugden, D. E. Late Quaternary glacial history of the George VI Sound area, West Antarctica. *Quat. Res.* **18**, 243–267 (1982).
8. Domack, E. W. *et al.* Late Holocene advance of the Müller Ice Shelf, Antarctic Peninsula: sedimentologic, geochemical, and palaeontological evidence. *Antarct. Sci.* **7**, 159–170 (1995).
9. Hjort, C., Bentley, M. J. & Ingólfsson, O. Holocene and pre-Holocene temporary disappearance of the George VI Ice Shelf, Antarctic Peninsula. *Antarct. Sci.* **13**, 296–301 (2001).
10. Pudsey, C. J. & Evans, J. First survey of Antarctic sub-ice shelf sediments reveals mid-Holocene ice shelf retreat. *Geol.* **29**, 787–790 (2001).
11. Brachfeld, S. *et al.* Holocene history of the Larsen-A Ice Shelf constrained by geomagnetic paleointensity dating. *Geology* **31**, 749–752 (2003).
12. Morris, E. M. & Vaughan, D. G. Glaciologic climate relationships spatial and temporal variation of surface temperature on the Antarctic Peninsula and the limit of viability of ice shelves. *Antarct. Res. Ser.* **79**, 61–68 (2003).
13. Scambos, T. A., Hulbe, C., Fahnestock, M. & Bohlander, J. The link between climate warming and break-up of ice shelves in the Antarctic Peninsula. *J. Glaciol.* **154**, 516–530 (2001).
14. King, J. *et al.* Antarctic Peninsula climate variability and its causes as revealed by analysis of instrumental records. *Antarct. Res. Ser.* **79**, 17–30 (2003).
15. Gilbert, R. & Domack, E. W. The sedimentary record of disintegrating ice shelves in a warming climate, Antarctic Peninsula. *Geochem. Geophys. Geosyst.* **4**, 1038, doi:10.2912002GC000441 (2003).
16. Domack, E. W., Jacobson, E. A., Shipp, S. S. & Anderson, J. B. Late Pleistocene-Holocene retreat of the West Antarctic Ice Sheet system in the Ross Sea: Part 2 – sedimentologic and stratigraphic signature. *Geol. Soc. Am. Bull.* **111**, 1517–1536 (1999).
17. MacAyeal, D. R., Scambos, T. A., Hulbe, C. & Fahnestock, M. A. Catastrophic ice-shelf break-up by an ice-shelf-fragment capsizing mechanism. *J. Glaciol.* **49**, 22–36 (2003).
18. Frank, M. *et al.* North Atlantic Deep Water export to the Southern Ocean over the past 14 Myr: evidence from Nd and Pb isotopes in ferromanganese crusts. *Paleoceanography* **17**, doi: 10.1029/2000PA000606 (2002).
19. Ishman, S. E. & Szymczek, P. Foraminiferal distributions in the former Larsen-A ice shelf and Prince Gustav Channel region, eastern Antarctic Peninsula margin: a baseline for Holocene paleoenvironmental change. *Antarct. Res. Ser.* **79**, 239–260 (2003).
20. Jacobs, S. S., Gordon, A. L. & Ardai, J. L. Jr. Circulation and melting beneath the Ross Ice Shelf. *Science* **203**, 439–445 (1979).
21. Gilbert, R., Domack, E. W. & Camerlenghi, A. Deglacial history of the Greenpeace Trough: ice sheet to ice shelf transition in the northwestern Weddell Sea. *Antarct. Res. Ser.* **79**, 195–204 (2003).
22. Shepherd, A., Wingham, D., Payne, T. & Skvarca, P. Larsen Ice Shelf has progressively thinned. *Science* **302**, 856–859 (2003).
23. Pahnke, K., Zahn, R., Elderfield, H. & Schultz, M. 340,000-year centennial-scale marine record of Southern Hemisphere climate oscillation. *Science* **301**, 948–952 (2003).
24. Norris, R. D., Park, B. K., Kang, S. H. & Khim, B. K. Stable isotope and ecological habitat of planktonic foraminifera adjacent to the ice edge in the western Weddell Sea. *Geosci. J.* **2**, 88–98 (1998).
25. Nicholls, K. W. *et al.* Water mass modification over the continental shelf north of Ronne Ice Shelf, Antarctica. *J. Geophys. Res.* **108**, doi:10.1029/2002JC001713 (2003).
26. Doane, S. S. *Oceanographic Observations in Front of the Larsen B Ice Shelf; Antarctica Prior to its Collapse in 2002*. BA thesis, Hamilton College (2003).
27. Scherer, R. P. A new method for the determination of absolute abundance of diatoms and other silt-sized sedimentary particles. *J. Paleolimnol.* **12**, 171–179 (1994).
28. Domack, E. W. *et al.* Marine sedimentary record of natural variability and recent warming in the Antarctic Peninsula. *Antarct. Res. Ser.* **79**, 205–224 (2003).
29. Evans, J. *et al.* Late Quaternary glacial history, flow dynamics and sedimentation along the eastern margin of the Antarctic Peninsula Ice Sheet. *Quat. Sci. Rev.* **24**, 741–774 (2005).

Supplementary Information is linked to the online version of the paper at www.nature.com/nature.

Acknowledgements This work was supported by grants from the National Science Foundation Office of Polar Programs. Timely support of analytical needs at the University of Arizona Accelerator Facility and the National Ocean Sciences Accelerator Mass Spectrometer laboratory was appreciated, as were the contributions of H. Schrum, E. Backman and K. Bart, and the comments by M. Canals, E. Rignot, L. Padman and T. Scambos.

Author Information Reprints and permissions information is available at npg.nature.com/reprintsandpermissions. The authors declare no competing financial interests. Correspondence and requests for materials should be addressed to E.D. (edomack@hamilton.edu).